TRANSIENT RESPONSE IN A DENDRITIC NEURON MODEL FOR CURRENT INJECTED AT ONE BRANCH

JOHN RINZEL *and* WILFRID RALL

From the Laboratory of Applied Studies, Division of Computer Research and Technology, and the Mathematical Research Branch, National Institute of Arthritis, Metabolism, and Digestive Diseases, National Institutes of Health, Bethesda, Maryland 20014

ABSTRACT Mathematical expressions are obtained for the response function corresponding to an instantaneous pulse of current injected to a single dendritic branch in a branched dendritic neuron model. The theoretical model assumes passive membrane properties and the equivalent cylinder constraint on branch diameters. The response function when used in a convolution formula enables one to compute the voltage transient at any specified point in the dendritic tree for an arbitrary current injection at a given input location. A particular numerical example, for a brief current injection at a branch terminal, illustrates the attenuation and delay characteristics of the depolarization peak as it spreads throughout the neuron model. In contrast to the severe attenuation of voltage transients from branch input sites to the soma, the fraction of total input charge actually delivered to the soma and other trees is calculated to be about one-half. This fraction is independent of the input time course. Other numerical examples, which compare a branch terminal input site with a soma input site, demonstrate that, for a given transient current injection, the peak depolarization is not proportional to the input resistance at the injection site and, for a given synaptic conductance transient, the effective synaptic driving potential can be significantly reduced, resulting in less synaptic current flow and charge, for a branch input site. Also, for the synaptic case, the two inputs are compared on the basis of the excitatory postsynaptic potential (EPSP) seen at the soma and the total charge delivered to the soma.

INTRODUCTION

To understand the passive integrative behavior of a neuron, we feel it is important to study the contribution made by individual input events. The steady-state aspect of such problems in an extensively branched neuron model was presented in a previous paper (Rall and Rinzel, 1973), hereafter referred to as RR-I. Symmetry, idealized branching, and linearity were exploited there to obtain analytical expressions for the steady membrane potential distribution in a branching neuron model for steady current input at a single dendritic branch site. These results were used to calculate the input resistance at branch terminal input sites and also to determine the steady-state voltage attenuation factor from a branch terminal input site to the soma. Here, we use the same superposition methods as in RR-I to solve the corresponding transient prob-

lem for arbitrary current injection at a single dendritic branch site. An explicit expression for the response function is obtained. We illustrate our results by calculating the transient potential at several locations in the neuron model for a particular transient current applied to a branch terminal. In addition, we discuss the reduction of synaptic driving potential associated with dendritic synaptic conductances and also the distribution of total charge dissipation for a transient current injection. More general response functions are derived in an appendix. We have also applied the results presented here in a theoretical study of dendritic spine function. This work will appear in a subsequent paper.

The applicability of this model to experimental neurons was discussed in RR-I. There we reviewed experimental evidence to show that cat spinal motoneurons satisfy the assumptions of the model to a reasonable approximation. The case for pyramidal tract neurons was also reviewed.

Previous transient solutions for dendritic neuron models have usually dealt with dendritic branches by lumping them together to avoid treating them individually. Those of Rall (1960) were obtained by using Laplace transform methods to treat dendritic cylinders of infinite length. Those of Rall (1962, 1969) defined a class of dendritic trees that can be treated as equivalent to cylinders of finite length, and used the classical method of separation of variables to treat a variety of initial conditions and boundary conditions. Studies of Jack and Redman (1971 a, b) have extended the application of Laplace transform methods to several difficult problems involving both cylinders of infinite length and cylinders of finite length. Recently, Redman (1973) has obtained the transient potential distribution in a neuron model which receives current in only some of its dendritic trees. Even these solutions, however, do not treat input at only a single branch of a tree. Transient results providing for segregation of input between four portions of the dendritic periphery were obtained in computations with compartmental models (Rall, 1964, Fig. 9). These results demonstrated that the membrane potential time course is the same at the soma (but not in the branches) for any apportionment of simultaneous current injection amongst the dendritic terminals, and that the amplitude at the soma depends only upon the total amount of this current. This property follows, of course, from the linearity of the system. Transient problems, for dendritic neuron models and membrane cylinders have also been treated by Lux (1967), MacGregor (1968), Barnwell and Cerimele (1972), and Norman (1972); transient input to a single location, with explicit treatment of branching, has been considered by Barrett and Crill (1974), and Butz and Cowan (personal communication).

Assumptions

We make the same assumptions here as in our previous paper (RR-I). Since a detailed discussion of these assumptions was provided there we will only summarize them here. Our neuron model is composed of N identical dendritic trees each of which exhibits M orders of symmetric branching. We assume that all branchings are symmetric bifurcations and that they satisfy the 3/2-power law, that is, each daughter branch diameter raised to the 3/2-power is equal to one-half times the 3/2-power of the parent branch
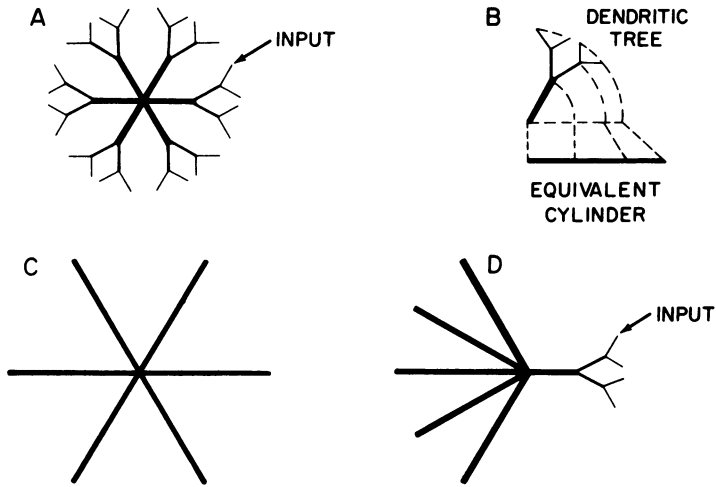
FIGURE 1   Diagrams illustrating features of the idealized neuron model. A represents the neuron model composed of six identical dendritic trees. B indicates the relation of a dendritic tree to its equivalent cylinder. C represents the same model as A, with each dendritic tree replaced by an equivalent cylinder. D represents the same model as A and C, with dendritic branching shown explicitly only for the tree which receives input current injected into the terminal of one branch; the five other trees of the model are represented by their equivalent cylinders, here shown gathered together. In diagrams A, C, and D, the point of common origin of the trees or equivalent cylinders is regarded as the neuron soma. Same as Rall and Rinzel (1973).

diameter. Hence, each tree is mathematically equivalent to a single membrane cylinder (Rall, 1962, 1964). Fig. 1 illustrates our branching neuron model with $N = 6$, $M = 2$ and the equivalent cylinder concept. Fig. 1 D should convey the following idea. When input is delivered to only one branch terminal in a single tree, the branching details of the other trees, which do not receive input directly, are unimportant. In the Appendix, we present solutions for problems with relaxed geometric assumptions.

Each trunk and branch segment in the neuron model is considered to be a cylinder of uniform passive membrane. The extracellular medium is taken to be isopotential; then, with the usual core conductor assumptions, we can treat each cylinder as a one dimensional, finite length, electrotonic cable. The membrane potential is continuous and core current is conserved at all branch points. The dendritic terminals, which do not receive applied current directly, are assumed to be sealed; that is, the membrane potential has zero slope with respect to axial distance at such terminals.

SYMBOLS

For Membrane Cylinders

$V_m = V_i - V_e$ Membrane potential, as intracellular minus extracellular electric potential; (volt).

$V = V_m - E_r$ Electrotonic potential, as deviation of membrane potential from its resting value E_r; (volt).

R_i	Resistivity of intracellular medium; (ohm centimeter).
R_m	Resistance across a unit area of membrane; (ohm centimeter^2).
C_m	Capacity of a unit area of membrane; (farad centimeter^{-2}).
d	Diameter of membrane cylinder; (centimeter).
$r_i = 4R_i/(\pi d^2)$	Core resistance per unit length; (ohm centimeter^{-1}).
$r_m = R_m/\pi d$	Resistance across a unit length of membrane; (ohm centimeter).
$c_m = \pi d C_m$	Membrane capacity per unit length; (farad centimeter^{-1}).
$\tau = R_m C_m$	Passive membrane time constant; (second).
t	Time; (second).
$T = t/\tau$	Dimensionless time variable.
p	Laplace transform variable for transform with respect to T.
$q = \sqrt{p + 1}.$	
$\tilde{F}(p)$	Laplace transform of $F(T)$.
$\lambda = [(R_m/R_i)(d/4)]^{1/2}$	Characteristic length of membrane cylinder, when extracellular resistance is neglected; (centimeter).
x	Actual distance along a cylinder axis; (centimeter).
$\Delta X = \Delta x/\lambda$	Increment of electrotonic distance; (dimensionless).
$X = \int_0^x (1/\lambda)\,dy;$	Electrotonic distance from origin; in a tree, λ changes at each branch point; (dimensionless).
L	Electrotonic distance from origin ($X = 0$) to the end of finite length cylinder ($X = L$).
$R_\infty = \lambda r_i = (2/\pi)(R_m R_i)^{1/2}(d)^{-3/2}$	Input resistance at origin of membrane cylinder of semi-infinite length; (ohm).
$K_{\text{ins}}(X, L, T)$	Response at time T and location X in a cylinder of length L *insulated* $(\partial V/\partial X = 0)$ at the origin for instantaneous point charge placed at the end $X = L$.
$K_{\text{clp}}(X, L, T)$	Response at time T and location X in a cylinder of length L *clamped* $(V = 0)$ at the origin for instantaneous point charge placed at the end $X = L$.
I	Transient current applied outward across membrane at $X = L$; (ampere).

For Idealized Neuron Model

N	Number of equivalent dendritic trees (or their equivalent cylinders) that are coupled at $X = 0$.
L	Electrotonic length of each of those trees or equivalent cylinders.
M	Number of orders of symmetric branching, specifically in the dendritic tree which receives the input.
X_1	Electrotonic distance from the origin to the first point of branching.
X_k	Electrotonic distance from the origin to the kth-order branch points.
$R_{T\infty}$	Input resistance for a dendritic *trunk* cylinder when extended for infinite length away from soma; (ohm).
R_N	Whole *neuron* input resistance at the point ($X = 0$) of

	common origin of the N trees or equivalent cylinders; (ohm).
R_{BL}	Input resistance at the end ($X = L$) of one terminal *branch* of the neuron model, for current applied as in Figs. 1 A and D; (ohm).
X_{in}	Electrotonic distance from the origin to the point of current injection.
I	Transient current applied outward across membrane at X_{in}; (ampere).
$K(X, T; X_{in})$	Response at time T and location X in the neuron model for instantaneous point charge placed at location X_{in}.

For the Discussion

I_p	Peak value of transient input current; Eq. 35; (ampere).
$V_{X;X_{in}}$	Transient depolarization at location X due to current injection at location X_{in}; (volt).
$W(X)$	Time integral of potential at location X; Eq. 40; (volt-second).
Q_{in}	Total input charge for a transient current injection; (coulomb).
$i_l(X, T)$	Current per unit length flowing across membrane leakage resistance; (ampere-centimeter^{-1}).
$q(X)$	Charge dissipation per λ length; (coulomb).
$Q(X_a, X_b)$	Total charge dissipated by membrane leakage in branch section from X_a to X_b; (coulomb).
V_{in}	Transient synaptic depolarization at some synaptic site, X_{in}; (volt).
g_ϵ	Synaptic excitatory conductance at this synaptic site; (ohm^{-1}).
$V_\epsilon = E_\epsilon - E_r$	Synaptic excitatory equilibrium potential, being the difference between the excitatory emf and the resting emf; (volt).
$(V_\epsilon - V_{in})$	Effective driving potential for excitatory synaptic current; (volt).
I_ϵ	Synaptic excitatory current; (ampere).

THEORY

For the usual assumptions of one dimensional cable theory, transient distributions of membrane potential along the length of a passive membrane cylinder must satisfy the partial differential equation:

$$\partial^2 V/\partial X^2 = (\partial V/\partial T) + V, \tag{1}$$

where X, T, and $V = V(X, T)$ are explicitly defined in the list of symbols. Our basic assumption is that this partial differential equation is satisfied in every trunk and branch cylinder of the idealized neuron model illustrated in Fig. 1.

The initial-boundary value problem for the injection of a time varying current, $I(T)$,

to a single branch terminal (Fig. 1 A and D), can be broken down into component problems (RR-I, Figs. 2 and 3). The overall problem consists of Eq. 1 together with an initial condition:

$$V(X, 0) = 0 \qquad (2)$$

for all trunks and branches, and with boundary conditions analogous to those of the steady-state problem. These boundary conditions can be stated as follows: $V(X, T)$ is continuous at the common origin and at all branch points ($X = X_k$); also there is conservation of current (Kirchhoff's law) at the origin and at all branch points; for the input branch, the terminal boundary condition can be expressed:

$$\partial V / \partial X = 2^M R_{T_\infty} I(T), \qquad \text{at } X = L, \qquad (3)$$

where $2^M R_{T_\infty}$ represents the R_∞ value (input resistance for semi-infinite length) of an Mth order branch (assuming symmetric branching which satisfies the equivalent cylinder constraint); for all other branch terminals, the boundary condition is simply:

$$\partial V / \partial X = 0, \qquad \text{at } X = L \qquad (4)$$

which represents a sealed end.

Solution as a Convolution of I(T) with a Response Function

Because we are dealing with a linear system, we know that the solution, $V(X, T)$ for $I(T)$ injected at one branch terminal can be formally expressed and also computed numerically in terms of the response function, $K(X, T; L)$, which is a function of T corresponding to the response at the location X, for an instantaneous point charge delivered at $T = 0$ at the input site, $X = L$, of one branch. The Appendix treats also other input sites, $X = X_{in}$, for which the response function is $K(X, T; X_{in})$. Here we express the transient solution, for $I(T)$ injected at $X = L$ of one branch, as the convolution:

$$V(X, T) = \int_0^T I(s) K(X, T - s; L) \, ds. \qquad (5)$$

The corresponding formula in the Laplace transform space is the product:

$$\tilde{V}(X, p) = \tilde{I}(p) \tilde{K}(X, p; L) \qquad (6)$$

where $\sim$ indicates Laplace transform with respect to T, and p is the transform variable. For examples and discussion, see Chapters XII and XIV of Carslaw and Jaeger (1959).

It is useful to comment on the relation between the response function and an instantaneous point charge represented in terms of the Dirac delta functions, $\delta(T)$ and $\delta(X)$. Consider an instantaneous point charge, Q_0 coulombs, applied at the terminal,

$X = L$, of one branch at $T = 0$. This can be treated as an input function:

$$I(T) = (Q_0/\tau)\delta(T) \qquad (7)$$

which is applied at $X = L$ of one branch. Then from Eq. 5, the resulting response can be expressed:

$$V(X, T) = (Q_0/\tau)K(X, T; L). \qquad (8)$$

It may be noted that Q_0/τ is in amperes, $K(X, T; L)$ is in ohms, and $V(X, T)$ is in volts; also, the factor (Q_0/τ) in Eq. 7, satisfies the condition that

$$\int_0^\infty I(t/\tau)\,dt = \tau \int_0^\infty I(T)\,dT = Q_0.$$

Normalization by setting $Q_0/\tau = 1$ A, means that $V(X, T)$ in volts has the same magnitude and dependence upon X and T as $K(X, T; L)$ in ohms. For an initial boundary value problem, we can alternatively set $I(T) = 0$ and regard the instantaneous point charge as an initial condition involving $\delta(X)$; if the instantaneous initial charge is Q_0 coulombs at the point $X = L$ of one branch, the initial condition in that branch can be expressed:

$$V(X, 0) = (Q_0/\lambda c_m)\delta(X - L)$$
$$= (2^M R_{T\infty} Q_0/\tau)\delta(X - L). \qquad (9)$$

Here it may be noted that λc_m is the membrane capacity per λ length of the terminal branch, and this times $V(X, 0)$, when integrated over X, yields Q_0 as the total initial charge. Also, the second expression follows from the first because

$$(\lambda c_m)^{-1} = (r_m/\lambda)/\tau, \text{ and } (r_m/\lambda) = 2^M R_{T\infty}$$

represents the input resistance for a semi-infinite length of the terminal branch cylinder, as in Eq. 3.

   For the present problem, the required response function consists of a sum of several component response functions, where each of these components corresponds to one of the components of the steady-state problem, as presented in (RR-I, Figs. 2 and 3). The correspondence between these components is made most apparent when the component initial-boundary value problems are expressed in the Laplace transform space, as illustrated in the next section.

Case of Cylinder Insulated at the Origin

For the single cylinder with current applied at $X = L$ and zero slope at $X = 0$ (see RR-I, Fig. 2 A), the initial-boundary value problem consists of Eqs. 1 and 2 together with:

$$\partial V / \partial X = R_{\infty} I(T), \qquad \text{at } X = L \tag{10}$$

and

$$\partial V / \partial X = 0, \qquad \text{at } X = 0. \tag{11}$$

Laplace transformation of Eq. 1 yields:

$$d^2 \tilde{V} / dX^2 = (p + 1) \tilde{V}, \tag{12}$$

which is an ordinary differential equation whose general solution can be expressed:

$$\tilde{V}(X, p) = A(p) \sinh(qX) + B(p) \cosh(qX), \tag{13}$$

where $q = (p + 1)^{1/2}$. Laplace transformation of Eq. 11 yields the boundary condition:

$$\partial \tilde{V} / \partial X = 0, \qquad \text{at } X = 0, \tag{14}$$

and this requires that $A(p) = 0$ in Eq. 13. It remains to determine $B(p)$ from the other boundary condition.

Laplace transformation of Eq. 10 yields the boundary condition:

$$\partial \tilde{V} / \partial X = R_{\infty} \tilde{I}(p), \qquad \text{at } X = L. \tag{15}$$

This, together with Eq. 13 and $A(p) = 0$, yields the solution:

$$\tilde{V}(X, p) = \frac{\tilde{I}(p) R_{\infty} \cosh(qX)}{q \sinh(qL)} \tag{16}$$

in the Laplace transform space, for this particular case.

Either by comparing Eq. 16 with Eq. 6, or by setting $I(T) = \delta(T)$, implying that $\tilde{I}(p) = 1$, we obtain the Laplace transform of the response function for this component problem, namely,

$$\tilde{K}_{ins}(X, L, p) = \frac{R_{\infty} \cosh(qX)}{q \sinh(qL)}. \tag{17}$$

Here, subscript "ins" designates this case of the cylinder insulated at the origin; also X designates the point where the response is observed, p is the complex variable of the Laplace transform domain, and L designates the electrotonic length of the component cylinder; it is assumed that current is injected at the end, $X = L$. When the point of observation is also set at $X = L$, then Eq. 17 simplifies to

$$\tilde{K}_{ins}(L, L, p) = (R_{\infty} / q) \coth(qL).$$

This particular Laplace transform has a formal correspondence with the input resis-

tance, $R_{CL,\text{ins}}$, and the input impedance, $Z_{CL,\text{ins}}$, of the steady-state presentation (RR-I, Eqs. 7 and A 15).

Case of Cylinder Clamped at the Origin

The other important special case will be presented more briefly. This is the case of a cylinder with $I(T)$ applied at $X = L$, and clamped at the origin ($V = 0$ at $X = 0$) corresponding to Fig. 2 B of the steady-state presentation. Here, Eqs. 1, 2, and 10 apply as before, and the clamped boundary condition at the origin requires that $B(p) = 0$ in Eq. 13. Then the boundary condition (Eq. 15) leads to the following Laplace transform of the response function for this component problem:

$$\tilde{K}_{\text{clp}}(X, L, p) = \frac{R_\infty \sinh(qX)}{q \cosh(qL)}. \tag{18}$$

This result for the clamped origin may be contrasted with Eq. 17 for the insulated origin. When $X = L$, this result corresponds formally to $R_{CL,\text{clp}}$ and the input impedance, $Z_{CL,\text{clp}}$, of the steady-state presentation (RR-I, Eqs. 9 and A 16). The next step is to combine these component results by means of superpositions corresponding to those of the steady-state presentation.

Result for Input Restricted to One Dendritic Branch Terminal

Given the two component results above, and reviewing the superpositions leading to (Eqs. 12 and 13 of RR-I) for N coupled cylinders and to (Eqs. 18–20 of RR-I) for the M orders of branching, we obtain the following general expression for the Laplace transform of the response function, for input restricted to one dendritic branch terminal,

$$\tilde{K}(X, p; L) = N^{-1}\tilde{K}_{\text{ins}}(X, L, p) + AN^{-1}\tilde{K}_{\text{clp}}(X, L, p)$$

$$+ \sum_{k=1}^{M} 2^{(k-1)}B_k\tilde{K}_{\text{clp}}(X - X_k, L - X_k, p), \tag{19}$$

where A and B_k are simple constants whose values are specified according to location, as follows:

in the input tree $\qquad\qquad A = N - 1$;
   in the input branch $\qquad\quad B_k = 1$, for all k from 1 to M;
   in the sister branch $\qquad\quad$ same, except $B_M = -1$;
   in the parent branch $\qquad\quad$ same, except $B_M = 0$;
   in the first cousin branches $\quad$ same, except $B_M = 0$, and $B_{M-1} = -1$;
   in the grandparent branch $\quad$ same, except $B_M = 0$, and $B_{M-1} = 0$;
$\qquad\qquad\qquad \cdots$
   in the input trunk $\qquad\qquad B_k = 0$, for all k;

in the other trees, $\qquad\quad \begin{cases} A = 1, \text{assuming, } X < 0, \text{ and} \\ B_k = 0, \text{for all } k. \end{cases}$

In this expression, all component response functions (Eqs. 17 and 18) have R_∞ set equal to $R_{T\infty}$.

Response Functions in the Time Domain

In the time domain, the response function, $K(X, T; L)$ for input restricted to one dendritic branch terminal is equal to the corresponding linear combination of component response functions. Thus, corresponding to Eq. 19 and using the notation introduced there, we have

$$
K(X, T; L) = N^{-1} K_{\text{ins}}(X, L, T) + A N^{-1} K_{\text{clp}}(X, L, T)
$$

$$
+ \sum_{k=1}^{M} 2^{k-1} B_k K_{\text{clp}}(X - X_k, L - X_k, T). \tag{20}
$$

This means that we can have a completely explicit expression for $K(X, T; L)$ as soon as we have explicit expressions for the two types of response functions, $K_{\text{ins}}(X, L, T)$ and $K_{\text{clp}}(X, L, T)$, in the time domain. These explicit expressions can be obtained by two quite different approaches. One is to invert the two Laplace transforms defined by Eqs. 17 and 18. These inverse transforms can be found in Roberts and Kaufmann (1966) expressed in terms of theta functions. The functional relations satisfied by the theta functions immediately give two representations for each response function. The other approach is to solve the component problems directly in the time domain. The response functions can again be represented in two ways. One way corresponds to solving the problem by separation of variables and the other by the method of images. The equivalence of the two representations is seen through an application of Poisson's summation formula (e.g., Carslaw and Jaeger, 1959).

The method of separation of variables has been previously applied to membrane cylinders by Rall (1969). To find the component response functions, we use his equations 17 and 30–32 with the initial condition $F(X) = R_\infty \delta(L - X)$ and obtain

$$
K_{\text{ins}}(X, L, T) = R_\infty \frac{e^{-T}}{L} \left\{ 1 + 2 \sum_{n=1}^{\infty} (-1)^n \cos(n\pi X/L) \exp[-(n\pi/L)^2 T] \right\}, \tag{21}
$$

and

$$
K_{\text{clp}}(X, L, T) = R_\infty \frac{2 e^{-T}}{L} \sum_{n=1}^{\infty} (-1)^{n-1} \sin\left(\frac{(2n-1)\pi}{2L} X\right) \exp\left[-\left(\frac{(2n-1)\pi}{2L}\right)^2 T\right]. \tag{22}
$$

These infinite series representations converge rapidly for large values of T. For small values of T, we make use of different representations which are based upon the fundamental solution

$$
V(X, T) = [Q_0 R_\infty / \tau(\pi T)^{1/2}] \exp[-(T + X^2/4T)] \tag{23}
$$

for an instantaneous point charge Q_0 placed at $X = 0$ of a semi-infinite ($0 \leq X \leq \infty$) membrane cylinder. It may be noted that $Q_0 R_\infty / \tau = Q_0/(\lambda c_m)$, because $\tau = r_m c_m$ and $R_\infty = r_m/\lambda$. For the case of a cylinder which extends infinitely in both directions from $X = 0$, half of the charge spreads in each direction, and the expression above is divided by 2; then this agrees with Hodgkin, as cited in Appendix I of Fatt and Katz (1951). The required representations, for small T, can be constructed by using the method of images (e.g., Carslaw and Jaeger, 1959). To satisfy the boundary condition, $\partial V/\partial X = 0$ at $X = 0$, equal instantaneous point charges are placed simultaneously, along an infinite line, at locations, $X = (2n - 1)L$ for all integer values of n. This superposition yields the response function,

$$K_{ins}(X, L, T) = R_\infty \frac{e^{-T}}{(\pi T)^{1/2}} \sum_{n=-\infty}^{\infty} \exp\{-[L(2n - 1) + X]^2/4T\}. \qquad (24)$$

Also, one obtains $V = 0$ at $X = 0$ by using instantaneous point charges of alternating signs at successive odd multiple locations, $X = (2n - 1)L$, along an infinite line; this superposition yields the response function,

$$K_{clp}(X, L, T) = R_\infty \frac{e^{-T}}{(\pi T)^{1/2}} \sum_{n=-\infty}^{\infty} (-1)^n \exp\{-[L(2n - 1) + X]^2/4T\}. \qquad (25)$$

These (small T) representations of the two response functions can be shown to be equivalent to the expressions derived and used by Jack and Redman (1971 a), provided one notes that their X corresponds to our $L - X$ (for the electrotonic distance between the input site and the point of observation), and that their summation of two expressions, over $n = 0$ to $n = \infty$, is equivalent to our summation of one expression over $n = -\infty$ to $n = +\infty$; then their Eq. 11 agrees with our Eq. 24, and their Eq. 14 agrees with our Eq. 25. While these two infinite series converge well for small values of T, they converge poorly for large values of T.

We have used the large time and small time representations to advantage in our calculations switching from one to the other in order to minimize computational effort. When $X = 0$ or $X = L$, the errors made in truncating the alternate representations for $K_{ins}(X, L, T)$ and $K_{clp}(X, L, T)$ are easily bounded. For example, with $X = L$, by neglecting all terms with $|n| > 1$ in Eqs. 24 and 25 when $T \leq 0.1$ for $L = 0.5$ and when $T \leq 0.5$ for $L = 1.5$, a relative error of no greater than 10^{-5} is committed. For the large time representations, Eqs. 21 and 22, the use of at least four terms when $T > 0.1$ for $L = 0.5$, and six terms when $T > 0.5$ for $L = 1.5$, will guarantee the same relative accuracy. We observe here that the number of terms needed for a given relative accuracy depends on the length L. In this sense, the small T representations can be also thought of as large L representations and similarly the large T representations can be thought of as small L representations.

ILLUSTRATIVE RESULTS AND DISCUSSION

Asymptotic Behavior of the Response Function at the Input Terminal

Useful physical intuitive insight can be obtained by considering the response function at the input terminal, in the time domain. When an instantaneous point charge, Q_0 coulombs, is placed at $X = L$ of the input branch, the earliest spread of charge occurs only within that one branch. During this very early time (before charge spreads into the parent branch and the sister branch) the voltage transient at the terminal must be identical with the early transient for Q_0 placed at the end of a semi-infinite cylinder whose R_∞ value is $2^M R_{T\infty}$. This early transient can be expressed (compare Eq. 23) as:

$$V(L, T) \sim (R_{T\infty} Q_0/\tau) 2^M \frac{e^{-T}}{(\pi T)^{1/2}} \text{ as } T \rightarrow 0, \tag{26}$$

where $\sim$ means "is asymptotic to."

As time goes on, the charge spreads and decays. If the membrane resistivity were infinite, there would be no dissipative charge decay, and the original charge Q_0 would spread and become distributed uniformly over the entire surface of the N dendritic trees of Fig. 1 A. The total membrane capacity of those trees equals that of the N equivalent cylinders (Fig. 1 C) and is $NL\lambda c_m$ where c_m is the membrane capacity per unit length of a trunk cylinder. Thus, the final uniform voltage (without dissipative decay) would be $Q_0/(NL\lambda c_m)$. However, because of finite membrane resistance, the charge redistribution is concurrent with charge decay (dissipative leak across membrane resistance). For very large values of time, the decaying voltage at the input terminal approaches that at all other locations; that is, for all X:

$$V(X, T) \sim \frac{Q_0}{NL\lambda c_m} e^{-T} = \left(\frac{R_{T\infty} Q_0}{\tau}\right) \frac{e^{-T}}{NL} \text{ as } T \rightarrow \infty \tag{27}$$

where the second expression makes use of the fact that $R_{T\infty} = r_m/\lambda$ and $\tau = r_m c_m$ together imply $R_{T\infty}/\tau = (\lambda c_m)^{-1}$. These physical intuitive considerations tell us that $V(L, T)$ begins as expression 26, but with spread of charge into other branches it departs from this transient function, and with further spread into all of the trees, it must finally approach expression 27; the complete solution must define the stages of transition from the early limiting case (26) to the final decay (27). This will now be shown to be the case.

If we set $X = L$ in Eqs. 20, 24, and 25, the response function at the terminal (for small T) is found to be:

$$\frac{K(L, T; L)}{R_{T\infty}} = \frac{e^{-T}}{N(\pi T)^{1/2}} \sum_{n=-\infty}^{\infty} \exp(-n^2 L^2/T)$$

$$+ \frac{(N-1)e^{-T}}{N(\pi T)^{1/2}} \sum_{n=-\infty}^{\infty} (-1)^n \exp(-n^2 L^2/T)$$

$$+ \frac{e^{-T}}{(\pi T)^{1/2}} \sum_{k=1}^{M} 2^{k-1} \sum_{n=-\infty}^{\infty} (-1)^n \exp[-n^2(L - X_k)^2/T]. \tag{28}$$

For each of the three infinite series in this expression, only the term for $n = 0$ does not vanish as $T \rightarrow 0$; then, noting that

$$\left(\frac{1}{N} + \frac{N-1}{N} + \sum_{k=1}^{M} 2^{k-1}\right) = 2^M,$$

we can write

$$\frac{K(L, T; L)}{R_{T_\infty}} \sim \frac{2^M e^{-T}}{(\pi T)^{1/2}} \text{ as } T \rightarrow 0. \tag{29}$$

This is seen to agree with the previous physical intuitive result (26) when normalized by setting $Q_0/\tau = 1.0$ A in Eq. 8.

To find the large time behavior of the response function at the terminal, we use the other representation. With $X = L$ in Eqs. 20–22, we have

$$\frac{K(L, T; L)}{R_{T_\infty}} = \frac{e^{-T}}{NL}\left\{1 + 2\sum_{n=1}^{\infty} \exp[-(n\pi/L)^2 T]\right\}$$

$$+ \frac{(N-1)e^{-T}}{NL} 2\sum_{n=1}^{\infty} \exp\left[-\left(\frac{(2n-1)\pi}{2L}\right)^2 T\right]$$

$$+ \frac{e^{-T}}{L}\sum_{k=1}^{M} 2^{k-1} \sum_{n=1}^{\infty} \exp\left[-\left(\frac{(2n-1)\pi}{2(L-X_k)}\right)^2 T\right]. \tag{30}$$

First, we note that these series fail to converge as $T \rightarrow 0$, because then each exponential term under each summation approaches unity. Then we note that as $T \rightarrow \infty$, each exponential term under each summation approaches zero. Therefore we can write

$$\frac{K(L, T; L)}{R_{T_\infty}} \sim \frac{e^{-T}}{NL} \text{ as } T \rightarrow \infty. \tag{31}$$

This agrees with the corresponding physical intuitive result (Eq. 27) when normalized by setting $Q_0/\tau = 1.0$ A in Eq. 8. Moreover, the same limit is obtained at any point X in the tree. This limit corresponds to the zero order ($n = 0$) term of a Fourier (cosine) series (see p. 1492 of Rall, 1969) and is independent of X; in other words, it corresponds to a component of potential that is uniformly distributed over the entire surface of the neuron model.

When T is neither too small nor too large, numerical computations with both representations (Eqs. 28 and 30) give identical results, to many significant figures. Fig. 2 illustrates this response function with the solid curve, for $M = 3$, $X_1 = 0.25$, $X_2 = 0.5$, $X_3 = 0.75$, $L = 1.0$, and $N = 6$. These parameters correspond to those used in the steady-state example of RR-I, Fig. 4. The upper dashed curve represents Eq. 29
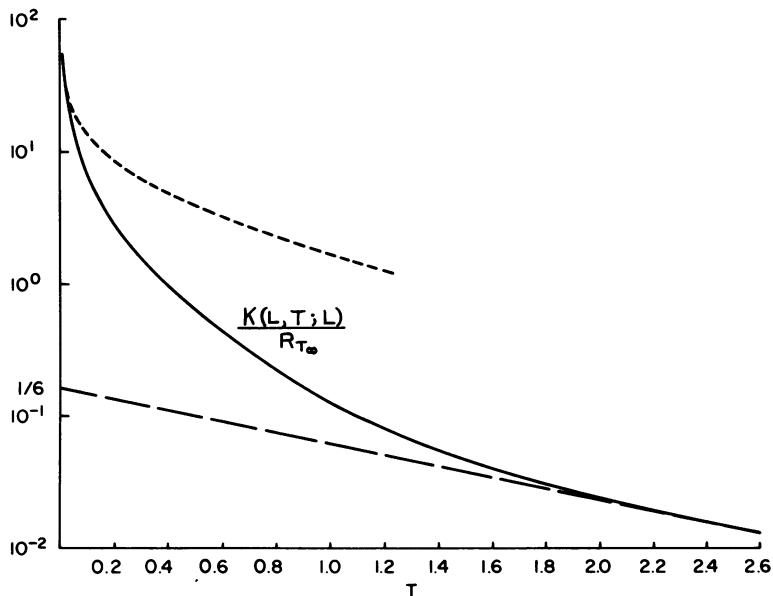
FIGURE 2 Response function at the input branch terminal (shown solid), compared with two asymptotic cases (shown dashed); ordinates are plotted on a logarithmic scale. The solid curve represents the response function defined by Eqs. 28 and 30 for $M = 3$, $X_1 = 0.25$, $X_2 = 0.5$, $X_3 = 0.75$, $L = 1.0$, and $N = 6$. The lower dashed curve is a straight line representing uniform decay and representing the asymptotic behavior of the response function as $T \rightarrow \infty$ (Eq. 31); its left intercept represents a value of $1/6$ because $NL = 6$. The upper dashed curve represents the asymptotic behavior as $T \rightarrow 0$ (Eq. 29); this also represents the response for a semi-infinite length of terminal branch. For any combination which makes $Q_0 R_{T_\infty} / \tau = 1$ mV, the values of the functions plotted here would correspond to V in millivolts; see Eqs. 26 and 27.

extended to all values of T. This full time course is valid for the limiting special case in which the length of the input branch is increased indefinitely. The earliest deviation of the solid curve from this dashed curve is due, physically, to the fact that when the spread of charge reaches the parent node $X = X_3$ its further spread is facilitated by the lower resistance provided by the parallel combination of the parent branch and the sister branch.

The lower dashed line in Fig. 2 represents Eq. 31, and it can be seen that the later decay of the solid curve agrees with this. The complications of spread over the entire surface of the neuron model, and the complications of the various infinite series in Eqs. 28 and 30 govern the precise way in which the solid curve transient passes from early agreement with the upper dashed curve to late agreement with the lower dashed curve.

The Response Function at X = 0

Here we state briefly the alternate representations in the time domain of the response function at the soma ($X = 0$) for input to a dendritic branch terminal. We recall that

772

for locations in the trunk of the input tree, the branching terms in Eq. 20 do not apply, and furthermore, when $X = 0$, the K_{clp} term must vanish. Therefore,

$$K(0, T; L) = (1/N) K_{ins}(0, L, T).\qquad(32)$$

For small values of T, we have the representation

$$K(0, T; L) = \frac{R_{T\infty} e^{-T}}{N(\pi T)^{1/2}} \sum_{n=-\infty}^{\infty} \exp\{-[L(2n - 1)]^2/4T\}\qquad(33)$$

which vanishes in the limit, as $T \to 0$. For T not too small, we have the representation

$$K(0, T; L) = \frac{R_{T\infty} e^{-T}}{NL} \left\{1 + 2\sum_{n=1}^{\infty} (-1)^n \exp[-(n\pi/L)^2 T]\right\}\qquad(34)$$

which agrees with Eq. 31 in the limit, as $T \to \infty$, as expected intuitively from Eq. 27.

It is important to realize that the response function evaluated at the origin is independent of the manner in which the input current $I(T) = \delta(T)$ is distributed among the branch terminals. More generally, for arbitrary current injections, the solution at $X = 0$ does not depend upon the way in which the input current is shared by locations which are electrotonically equidistant from the soma.

Illustrative Transients Computed by Convolution

Figs. 3–5 illustrate voltage transients computed according to the convolution formula (5) for several different locations in the neuron model, when one particular current transient was applied to a single branch terminal. The neuron model parameters were $N = 6$, $M = 3$, and with all of the same branch lengths as in RR-I, Fig. 4. The input current, $I(T)$, had a time course of the form

$$I(T) = I_p \alpha T e^{(1-\alpha T)}\qquad(35)$$

with $\alpha = 50$. This input function has a smooth time course, starting from $I = 0$ at $T = 0$, reaching a peak value of I_p at $T = (1/\alpha) = 0.02$, returning halfway down at about $T = 2.7/\alpha = 0.054$, and being effectively zero from $T = 0.15$ onwards. The graph of Eq. 35 with $I_p = 1$ A, appears in Fig. 3. This function is the same as the "fast input transient" used previously (Rall, 1967). This family of input transients has also been used extensively by Jack and Redman (1971 *a, b*). As mentioned previously, we have employed both the small time and large time component response functions in our calculations. To evaluate convolutions of Eq. 35 with the small time representations, we used a technique described by Jack and Redman (1971 *a;* pp. 312–313).

In Fig. 3, the upper dashed curve shows the input current time course and the solid curve shows the resulting voltage transient at the input branch terminal. Here, a linear voltage amplitude scale has been used, and the attenuated soma voltage transient
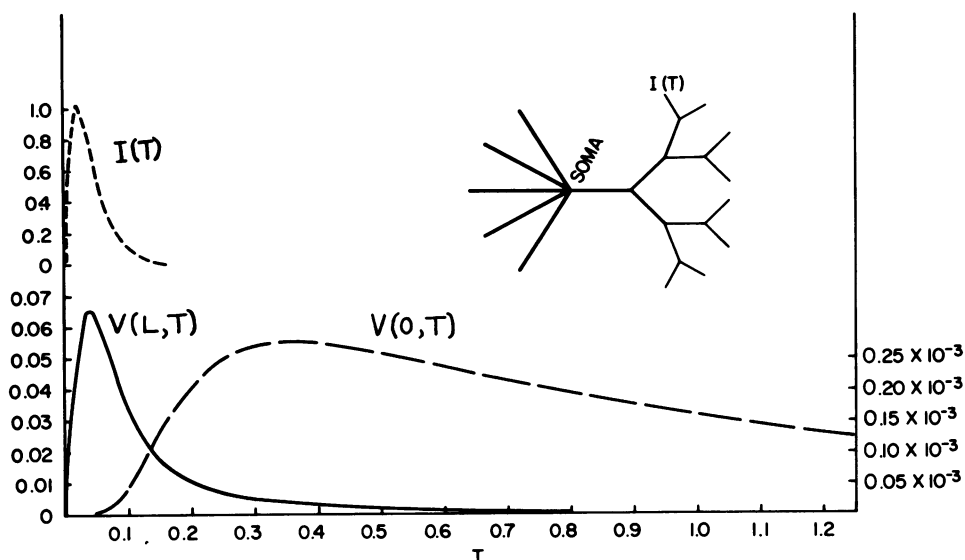
FIGURE 3 Computed voltage time course at the input receiving branch terminal (solid curve) and at the soma (lower dashed curve) for a particular time course, $I(T)$, of injected current (upper dashed curve). $I(T)$ is given by Eq. 35 with $\alpha = 50$ and shown here as $I(T)/I_p$. The neuron model is shown upper right and the parameters used were $N = 6$, $M = 3$, $X_1 = 0.25$, $X_2 = 0.5$, $X_3 = 0.75$, and $L = 1$. The ordinate values for the solid curve, using scale at left, represent dimensionless values of $V(L, T)/(2^M R_{T_\infty} I_p e)$ where $V(L, T)$ was obtained using Eqs. 5, 28, 30, and 35. The soma response (lower dashed curve) has been amplified 200 times; the ordinate values, using scale at right, represent dimensionless values of $V(0, T)/(2^M R_{T_\infty} I_p e)$ where $V(0, T)$ was obtained using Eqs. 5, 33, 34, and 35. The factor $2^M R_{T_\infty} I_p e$ equals $8 \times (4.56\ R_N) \times (I_p e)$ which is approximately equal to 100 times the product R_N and I_p. For example, if $R_N = 10^6\ \Omega$ and $I_p = 10^{-8}$ A, the above factor is approximately 1 V; then the left-hand scale can be read in volts for $V(L, T)$ and the right-hand scale can be read in volts for $V(0, T)$.

(lower dashed curve) has been amplified 200 times to aid visual comparison of these voltage response shapes. In Fig. 4, the same two voltage transients have been replotted to a log amplitude scale, together with transients at other locations. This permits comparison for successive locations along the main line from the input branch terminal (BI), to the parent node (P), to the grandparent node (GP), to the greatgrandparent node (GGP), and to the origin ($X = 0$, or soma) of the model. Also included is the further attenuated and delayed transient predicted for the branch terminals of the five other trees (OT) which do not contain the input branch. It can be seen that with increasing electrotonic distance from the input terminal, the time of the peak becomes increasingly delayed and the peak amplitude becomes increasingly attenuated. These peak times, amplitudes and attenuation factors have been collected in Table I. Each transient attenuation factor represents the ratio of peak $V(L, T)$ to the peak V at the location in question; these transient attenuation factors are all greater than those for the steady-state problem, which are included in the bottom row of Table I, for comparison. It should be emphasized that these particular values depend upon
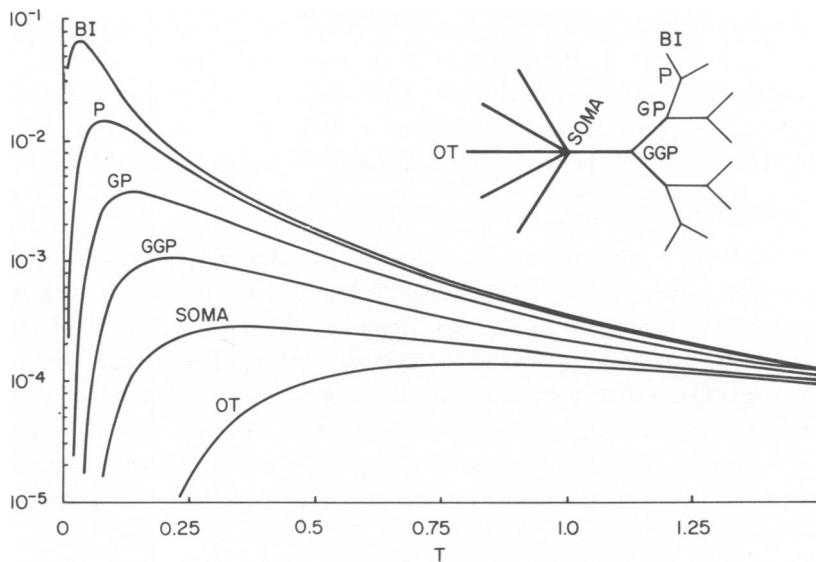
FIGURE 4 Semi-log plots of transient membrane potential versus T at successive sites along the mainline in the neuron model for transient current injected into the terminal of one branch. BI designates the input branch terminal while P, GP, and GGP designate the parent, grandparent, and great grandparent nodes, respectively, along the mainline from BI to the soma. The response at the terminals of the trees not receiving input directly is labeled OT. The model parameters, neuron branching diagram, and current time course are the same as in Fig. 3. Also as in Fig. 3, the ordinate values represent dimensionless values of $V(X, T)/(2^M R_{T_\infty} I_p e)$ where $V(X, T)$ was obtained as the convolution of $I(T)$ with $K(X, T; L)$ defined by Eqs. 5, 20, and 35 using 21, 22, 24, and 25.

the particular values of $N = 6$, $M = 3$, $L = 1$ with $\Delta X = 0.25$, and the particular input transient used. A faster input transient would result in larger transient voltage attenuation factors, while a slower input transient would result in smaller factors, with the steady-state values as a lower limit; see Fig. 3 of Redman (1973) for an illustration of this point. In Table I, the transient attenuation factor of 235 (from BI to soma) is nearly 10 times the factor, 23.9, for the steady-state case.

It may be noted that both of these attenuation factors can be attributed partly to electrotonic distance and partly to branching. This can be demonstrated by comparison with results obtained without branching (or with input current divided equally

TABLE I

TRANSIENT ATTENUATION FACTORS AND PEAK TIMES FROM FIGS. 4 AND 5, AND STEADY-STATE ATTENUATION FACTORS FROM (RR-I, FIG. 4)

Location:	BI	P	GP	GGP	Soma	BS	BC-1	BC-2	OT
Peak time	0.04	0.085	0.135	0.21	0.35	0.12	0.27	0.46	0.84
Peak value × 10³	64.8	14.5	3.75	1.05	0.276	12.8	2.54	0.557	0.135
Transient attenuation factor	1.0	4.5	17.3	62	235	5.1	25	116	479
Steady-state attenuation factor	1.0	2.3	5.3	12.0	23.9	2.4	6.0	15.5	34.0

among the eight branch terminals of one tree). Then, for the same input current time course (α = 50 in Eq. 35) the response at the soma is the same as before, but the voltage at the input terminals is reduced. .The transient attenuation factor is reduced to 30.3 and the steady-state factor is reduced to 6.02; these reduced values represent attenuation attributable solely to electrotonic distance, and not to branching.

Transients at All Branch Terminals.

In Fig. 5, all of the voltage transients correspond to branch terminals ($X = L$), and the comparison is between the input branch terminal (BI), its sister branch terminal (BS), the first and second cousin branch terminals (BC-1) and (BC-2) of the same dendritic tree (see diagram of neuron model), as well as all terminals of the other dendritic trees (OT). It can be seen that the sister transients (BI and BS) become effectively identical from $T = 0.25$ onward; also this joint transient later becomes effectively identical with the transient (BC-1) from $T = 0.75$ onwards. These effects can be intuitively understood as due to rapid equalizing electrotonic spread between neighboring branches.

Also, it can be seen in Figs. 4 and 5, and verified in Table I, that both the peak time and the attenuation factor of the sister terminal (BS) exceed the values for the parent node (P), as should be expected from the intuitive consideration that the spread of charge must reach the parent node before it can spread into the sister branch. It is
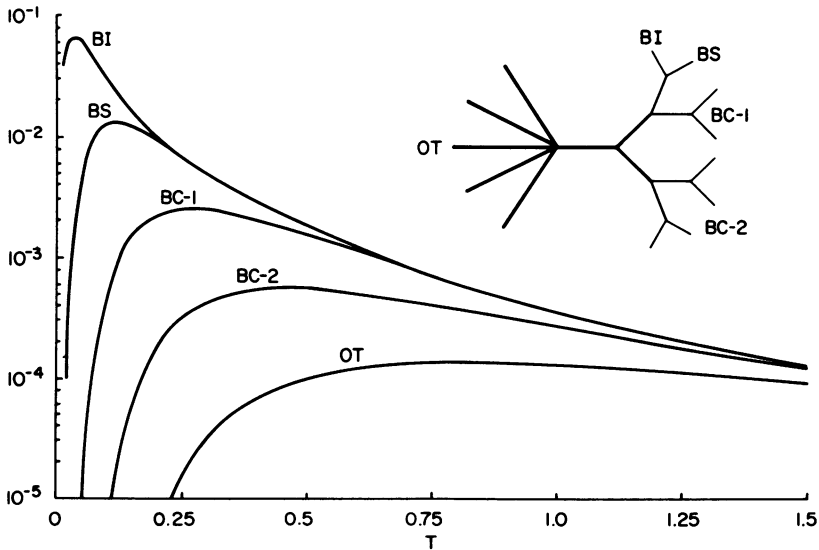

FIGURE 5 Semi-log plots of voltage versus T at all of the branch terminals in the neuron model for transient current injected into the terminal of one branch. Refer to Fig. 3 for model parameters and input current parameters. BI and BS designate the input branch terminal and the sister branch terminal. BC-1 and BC-2 designate the terminals of the two first cousin and the four second cousin branches in the input tree, while OT designates the branch terminals of the other five trees. The transients are computed and scaled as indicated in Fig. 4.

noteworthy that in both the transient and in the steady state, the attenuation from BI to P is much greater than that from P back out to BS. In the steady-state results (RR-I, Fig. 4) this is an obvious result of the fact that the zero slope boundary condition at the sister terminal (BS) tends to minimize attenuation, while the relatively large current flows at the parent node (P) permit steep gradients and large attenuation. Similar statements can be made about the first cousin terminals (BC-1) following the grandparent node (GP), and about (BC-2) following (GGP), and (OT) following soma.

Transient Peak Depolarization Not Proportional to Input Resistance

This section is concerned with current injection only; additional complications associated with synaptic membrane conductance are treated in a separate section. We will compare the case of membrane depolarization at a dendritic branch terminal when current is injected only there, with the reference case of membrane depolarization at the soma when the same current is injected only at the soma. For steady current, it follows from the definition of input resistance, that the ratio of the steady depolarizations obtained in these two cases must equal the ratio, R_{BL}/R_N, of the input resistances at these two sites. However, for brief transient input current, it is not the two input resistances but the response functions at the two input sites that must be considered; this has been noted earlier in RR-I and Redman (1973). It is the convolution of $I(T)$ with the response function $K(L, T; L)$ for the case of branch terminal input, which is to be compared with the reference case provided by convolution of the same $I(T)$ with the response function $K(0, T; 0)$ at the soma for input at the soma.

Such a comparison is illustrated by the solid curves of Fig. 6, which were computed for the same neuron model parameters and the same brief current transient as before (see figure legend for specifics). Here, the ratio of the peak depolarizations, peak $V_{L;L}$/peak $V_{0;0}$, is equal to 46.3; this is nearly three times the ratio of the input resistances, $R_{BL}/R_N = 15.5$, that was calculated for the same model parameters (RR-I, p. 667). It should also be emphasized that $V_{L;L}(T)$ and $V_{0;0}(T)$ have no overall constant of proportionality because of their difference in time course; this is seen by means of the dashed curves in Fig. 6, which rescale the amplitude of $V_{0;0}(T)$ by the factor, 15.5 for the lower dashed curve, and by the factor, 48, for the upper dashed curve. It can be seen that the half-width of this soma response time course is more than 3/2 that of $V_{L;L}(T)$. The more rapid response at a branch terminal can be understood in terms of the rapid equalization between neighboring branches.

To understand why the peak depolarizations at the two input sites scale as they do, we consider the asymptotic behavior (as $T \to 0$) of the corresponding response functions. The small time expression for the response function at a terminal input location $K(L, T; L)$ is given by Eq. 28 and its asymptotic form (as $T \to 0$) is expressed by Eq. 29. For the soma, the small time expression for $K(0, T; 0)$ is given by Eq. (54) in the Appendix, and its asymptotic form can be expressed

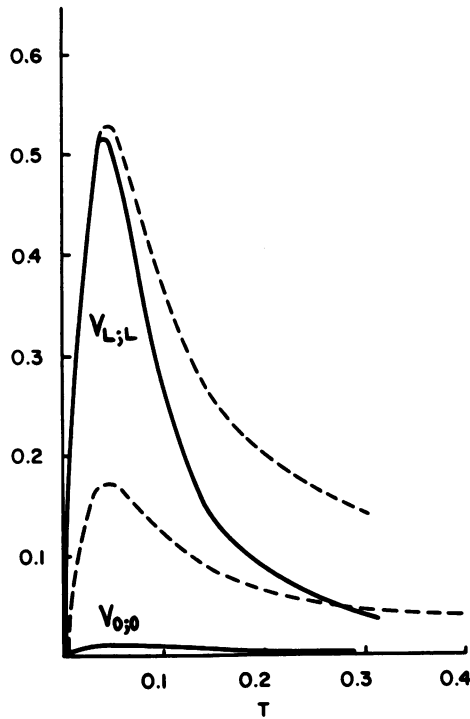$$\frac{K(0, T; 0)}{R_{T_\infty}} \sim \frac{e^{-T}}{N(\pi T)^{1/2}} \text{ as } T \to 0. \tag{36}$$

FIGURE 6 Voltage transients (shown solid) versus T at two different sites of current injection. The upper solid curve $V_{L;L}(T)$ is the voltage transient at $X = L$ for current injection to that branch terminal; it is obtained as the convolution of $I(T)$ with $K(L, T; L)$, given by Eqs. 28 and 30. The lower solid curve $V_{0;0}(T)$ is the response at the soma when the same current is applied there; it is obtained as the convolution of $I(T)$ with $K(0, T; 0)$, given by Eqs. 53, 54, and 21. The model neuron parameters and current time course agree with those used in Fig. 3. The ordinate values represent dimensionless values of $V/(I_p e\ R_{T_\infty})$. The lower dashed curve is $V_{0;0}(T)$ times 15.5 which is the ratio, R_{BL}/R_N of the input resistance at the branch terminal to that at the soma. The upper dashed curve is $V_{0;0}(T)$ times 48 which is equal to $N2^M$ for $N = 6$, $M = 3$.

Because 29 and 36 have the same time dependence, we can express the limiting ratio of these response functions simply as

$$\lim_{T \to 0} \left\{ \frac{K(L, T; L)}{K(0, T; 0)} \right\} = N2^M. \tag{37}$$

This ratio equals 48 for our example ($N = 6$ with $M = 3$). It follows from Eq. 37 that for very small values of T, $V_{L;L}(T)/V_{0;0}(T) \sim N2^M$, for the case of a branch terminal input site compared with a soma input site. When $I(T)$ is very brief, this makes the peak values of $V_{L;L}(T)$ and $V_{0;0}(T)$ occur early, and it follows that the ratio, peak $V_{L;L}$/peak $V_{0;0}$ will also be close to $N2^M$. This explains the peak ratio of 46.3 in Fig. 6 being close to the limiting value of 48. For slower $I(T)$, the peak values of $V_{L;L}(T)$ and $V_{0;0}(T)$ occur later, Eq. 37 does not apply, and the peak ratio is ex-

pected to be smaller; for very slow $I(T)$, the ratio, $V_{L;L}/V_{0;0}$, approaches the steady-state ratio, R_{BL}/R_N, of 15.5 for this case. The physical intuitive explanation of Eq. 37 is that at very early times, both input locations respond like the origin of a semi-infinite cylinder, and it may be noted that the response function of a semi-infinite cylinder scales as $d^{-3/2}$. The branch terminal $d^{3/2}$ value is 2^{-M} times that of a trunk of this model, while at the soma, the N trunks provide a combined $d^{3/2}$ value which is N times that of a single trunk; this implies a $d^{3/2}$ ratio of $N2^M$ which agrees with the limiting response function ratio of Eq. 37.

Before leaving this subject, we note that here we have compared different input sites which have response functions of quite different time course. If, instead, we compare input sites at the somas of two neurons or neuron models of different size but having equal L (and equal ρ if the lumped soma is considered), then the two response functions have the same time course and their relative magnitudes correspond to their input resistance ratio. Similarly, input sites on two different cylinders of infinite length ($\pm\infty$) would also have response functions whose relative magnitudes correspond to their input resistance ratio; cf., Katz and Thesleff (1957); also, Katz and Miledi (1963). But for the general case of different input sites having different response functions (of different time course), it is clear that the early portions of the responses to brief input will not exhibit the input resistance ratio.

Comment Contrasting This Ratio with Attenuation Factor

In the preceding section, we considered the voltage peak ratio, peak $V_{L;L}/$peak $V_{0;0}$ which had a value of 46.3 in the example illustrated in Fig. 6. This peak ratio should be distinguished from the transient attenuation factor (from branch terminal to soma), the ratio, peak $V_{L;L}/$peak $V_{0;L}$, and which has a value of 235 in Figs. 3 and 4, and Table I. It should be noted that for a given $I(T)$, the numerator, peak $V_{L;L}$, is the same in both ratios, but the denominators are different: peak $V_{0;L}$ is the delayed and attenuated peak at the soma for input at the dendritic terminal, while peak $V_{0;0}$ is the early peak at the soma for a separate input at the soma.

Ratios of Time Integrals of Voltage Transients

It is well known that when the applied current, $I(T)$, is prolonged and approaches a steady current, then the relative voltage amplitudes at different locations approach their relative steady-state voltage values. It is less well known, but it has been noted both by Redman (1973) and by Barrett and Crill (1974) that these steady-state relative values also hold for the time integrals of brief voltage transients, provided that these are produced by the same transient $I(T)$. To be completely explicit, this means for the present study, that

$$\frac{\displaystyle\int_0^\infty V_{L;L}(T)\,\mathrm{d}T}{\displaystyle\int_0^\infty V_{0;0}(T)\,\mathrm{d}T} = \frac{R_{BL}}{R_N}, \tag{38}$$

and that

$$\frac{\int_0^\infty V_{L;L}(T)\,dT}{\int_0^\infty V_{0;L}(T)\,dT} = \frac{R_{BL}\cosh L}{R_N}. \tag{39}$$

The last ratio represents the steady-state attenuation factor (from branch terminal to soma) of our previous paper (RR-I, Eqs. 24–26).

The easiest way to justify these assertions about the ratios of time integrals of voltage for transient $I(T)$ will also serve to prepare the way for the next section which deals with the distribution and dissipation of membrane charge over the neuron model.

We define the time integral of $V(X, T)$ as

$$W(X) = \tau \int_0^\infty V(X, T)\,dT. \tag{40}$$

If $I(T)$ has a finite duration, such that $V(X, T) = 0$ at $T = 0$ and at $T = \infty$, it follows that integration of $\partial V/\partial T$ from $T = 0$ to $T = \infty$ must equal zero because $V = 0$ at both limits of integration. This means that integration of each term in the partial differential equation (Eq. 1) from $T = 0$ to $T = \infty$ yields the ordinary differential equation

$$d^2 W/dX^2 - W = 0. \tag{41}$$

This means that $W(X)$ satisfies the corresponding steady-state problem in all branches of the neuron model, and it follows that Eqs. 38 and 39 above must hold. The boundary condition at the input terminal can then be expressed

$$dW/dX = 2^M R_{T\infty} Q_{in} \text{ at } X = L, \tag{42}$$

where

$$Q_{in} = \tau \int_0^\infty I(T)\,dT \tag{43}$$

is the total input charge delivered by the transient input current.

Distribution of Charge Dissipation in the Dendritic Model

The total input charge is dissipated by leakage across the passive membrane resistance of the entire neuron model, because portions of this charge spread from the terminal along the dendrites to the soma and into the other dendritic trees of the model during

the time that charge dissipation takes place. Questions about how this charge dissipation is distributed over dendrites and soma have been posed and discussed by Redman (1973), Iansek and Redman (1973), and by Barrett and Crill (1974). Here we present the results obtained for our particular neuron model.

At any location in the model, charge is dissipated by the leakage current

$$i_l = V/r_m \qquad \text{amperes per centimeter,}$$

which represents a current density per unit length of the cylinder in question. For a location in a kth order branch of the model, the charge dissipation current per λ length, can be expressed

$$\lambda i_l = \lambda V/r_m = V/(2^k R_{T_\infty}) \qquad \text{amperes per } \lambda, \tag{44}$$

where $(2^k R_{T_\infty})^{-1} = \lambda/r_m$ is the membrane conductance per λ length in a kth order branch.

The time integral of this current provides $q(X)$, the total charge dissipation per λ length, at the location X; using Eqs. 40 and 44, this can be expressed

$$q(X) = \tau \int_0^\infty \lambda i_l dT = \frac{W(X)}{2^k R_{T_\infty}} \qquad \text{coulombs per } \lambda. \tag{45}$$

It may be noted that $q(X)$ can also be expressed

$$q(X) = \lambda c_m \int_0^\infty V(X, T) \, dT \tag{46}$$

where λc_m represents the membrane capacity per λ length of the cylinder in question; because $\lambda \propto d^{1/2}$ and $c_m \propto d$, it follows that $\lambda c_m \propto d^{3/2}$, and for symmetric branching with the equivalent cylinder constraint $d_k^{3/2} \propto 2^{-k}$, implying that $\lambda c_m \propto 2^{-k}$ in Eq. 46, in agreement with Eq. 45.

Because the scaling factor in Eq. 45 depends on position X in the neuron model, we see that the dependence of $q(X)$ upon X is different from that of $W(X)$ and, hence, different from that of a steady-state potential distribution. To be completely explicit, this means, for brief $I(T)$ injected at a dendritic terminal, the ratio of $q(L)$ at the terminal to $q(0)$ at the soma (per λ length of one dendritic tree trunk) can be expressed

$$q(L)/q(0) = (R_{BL} \cosh L)/(2^M R_N). \tag{47}$$

For our specific example ($N = 6, M = 3, L = 1, \Delta X = 0.25$), this means that the steady-state attenuation factor (Eq. 39) of 23.9, is divided by 8 to obtain a value slightly less than 3 for the charge dissipation ratio of Eq. 47. The physical intuitive reason why the charge dissipation ratio (Eq. 47) is smaller than the voltage ratio (Eq. 39) is that

the terminal branch has a smaller membrane capacity per λ length than does the dendritic trunk; see Eq. 46 and comments attached to it.

Total Charge Dissipation in Each Branch

The amount of total charge dissipation in a segment of a kth order branch, from X_a to X_b, can be expressed,

$$
\begin{aligned}
Q(X_a, X_b) &= \int_{X_a}^{X_b} \mathfrak{q}(X)\,\mathrm{d}X \\
&= (2^k R_{T\infty})^{-1} \int_{X_a}^{X_b} W(X)\,\mathrm{d}X \qquad (48) \\
&= (2^k R_{T\infty})^{-1}\left(\left.\frac{\mathrm{d}W}{\mathrm{d}X}\right|_{X_b} - \left.\frac{\mathrm{d}W}{\mathrm{d}X}\right|_{X_a}\right),
\end{aligned}
$$

where use has been made of Eq. 45 and the integration makes use of Eq. 41. The last expression represents exactly the difference between the total charge which has flowed into the cylinder at X_a and out of the cylinder at X_b, i.e., the difference of the core currents integrated over time. As a consequence of Eq. 41 we see that $Q(X_a, X_b)$ can be determined merely by evaluating derivatives of W. It is important to realize that $\mathfrak{q}(X)$, and hence any integral of $\mathfrak{q}(X)$, is independent of the time course of the transient input current. Moreover, the fraction of total input charge dissipated in the segment X_a to X_b is given by the ratio, $Q(X_a, X_b)/Q_{in}$. This fraction exhibits no dependence upon input time course, provided that $V(X,0) = 0 = V(X, \infty)$; in other words, it depends only upon geometric and electrotonic parameters. Also, at the soma and in the dendritic trunks, $\mathfrak{q}(X)$ is independent of the way in which $I(T)$ might be distributed among one or more sites at the same electrotonic distance from the soma in that tree. Redman (1973) and Iansek and Redman (1973) have made a similar observation regarding the amount of charge which reaches the soma in their theoretical model.

For illustrative purposes, we have computed the fraction of total input charge dissipated in various portions of our neuron model when input is restricted to a single branch terminal. The results of our calculations are displayed in Fig. 7 as percentages. We find that the portion of charge dissipated along the mainline from the input site to the origin is $7.6 + 6.6 + 5.7 + 5.3$, or about 25%. The portion dissipated in the side branches off the mainline is $4.5 + 7.4 + 9.1$, or about 21%. Thus, combining the mainline with the side branches, the entire input tree dissipates about 46% of the total input charge. The portion dissipated in the other trees (5×10.8) equals 54% of the total. These figures account for 100% of the charge dissipation; however, if we designate a finite soma surface area composed of six initial length increments, $\Delta X = 0.1$, one from each dendritic trunk, it follows that this soma surface dissipates about 8.5% of the total input charge.

At first, it may seem surprising that half of the total input charge spreads from the input tree through the soma into the other trees, to be dissipated there. This may seem
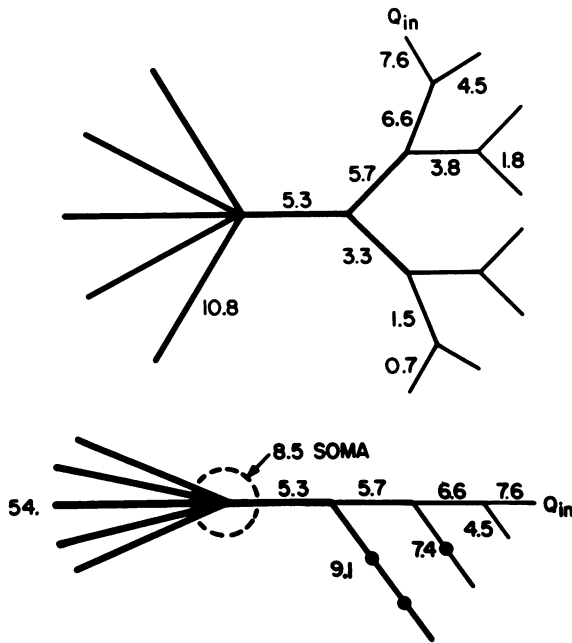
FIGURE 7 Diagrams illustrating percentages of total input charge Q_{in} dissipated in different branches of the neuron model for transient current injection at a single branch terminal. The model neuron parameters agree with those of Fig. 3. The upper diagram indicates the distinct percentages dissipated in various branches of the input tree. For those branches which dissipate equal percentages of Q_{in}, that percentage is indicated only once, e.g., each second cousin branch claims 0.7% of Q_{in}. The lower diagram shows the percentage of Q_{in} dissipated in the various side paths which leave the mainline from the input site to the origin. Also indicated is the percentage 8.5% of Q_{in} dissipated in a soma which corresponds to the segment of $X = 0$ to $X = 0.1$ of each trunk. The percentages are calculated using Eq. 48 and (RR-I, Eq. 20 where V and I are replaced by W and Q_{in}, respectively).

to conflict with the large transient peak attenuation factors; 235 from input terminal to soma, and 479 from input terminal to other trees (see Fig. 4 and Table I). One must remember, however, that charge dissipation at different locations is quite different from the transient voltage peaks for two reasons: (1) it is not the voltage peak but the time integral of voltage that is important here, and these $W(X)$ values relate to steady-state voltage attenuation (see Eqs. 40 and 41); (2) the relative values of membrane capacity per λ length further reduce the steady-state voltage ratios to give total charge dissipation ratios. It may be noted that the ratio of capacity per λ length of $(N - 1)$ other trees to that of the terminal branch equals $(N - 1)2^M$, or 40 in our example of $N = 6, M = 3$, (see Eqs. 45–47).

Which is most important, the low charge dissipation ratio, the moderate steady-state voltage attenuation factor, or the larger transient voltage peak attenuation factor? It depends upon the situation and the focus of concern. When one is concerned about the nonlinear effects of combining several synaptic inputs treated as synaptic conduc-

tance changes the voltage at the input sites is very important; attempts to estimate this from observations at the soma involve estimation of the transient voltage peak attenuation factor. On the other hand, when such nonlinear effects are shown or assumed to be unimportant, and one wishes to compare contributions of synapses at different locations, it can be useful to do this in the context of several input charges, and total charge dissipation. However, one must add the caution that such considerations of total charge dissipation completely disregard temporal considerations such as input time course and relative timing of several inputs; see (Rall, 1964, Fig. 7) for an illustration.

Synaptic Membrane Conductance Change as Input

In our previous paper (RR-I), we pointed out that synaptic depolarization at the input site should not be expected, in general, to be proportional to the input resistance at the synaptic site, and a steady-state illustration was provided. Here we will give the promised illustration and discussion for transients. There are two important factors.

One factor is often referred to as synaptic nonlinearity; when there is significant synaptic depolarization of different amounts at two synaptic sites, equal conductance transients do not produce equal synaptic current; this is explained and illustrated below. The other factor is the difference between the response functions at different input sites; this has been discussed above with Eq. 37 and Fig. 6.

For a transient excitatory membrane conductance, $g_\epsilon(T)$, the synaptic current $I_\epsilon(T)$ is given by

$$I_\epsilon(T) = g_\epsilon(T)[V_\epsilon - V_{in}(T)], \tag{49}$$

where V_ϵ is the synaptic equilibrium potential, assumed constant, and $V_{in}(T)$ is the transient depolarization at the input site X_{in}. Explanation and discussion of how this equation relates to the membrane equivalent circuit can be found in earlier papers (Rall, 1962, 1964); there G_ϵ was used to represent g_ϵ per unit area. The important point to notice is that membrane depolarization (increase of V_{in} from its zero resting value) reduces the effective synaptic driving potential, $V_\epsilon - V_{in}$, during the temporal variation of g_ϵ; consequently, less synaptic current flows than would have flowed if V_{in} did not change in Eq. 49.

The solution in all parts of the neuron model can be expressed in terms of the response function $K(X, T; X_{in})$ for current input at X_{in}. In particular, the solution at X_{in} satisfies

$$V_{in}(T) = \int_0^T I_\epsilon(s) K(X_{in}, T - s; X_{in}) \, ds.$$

The convolution on the right defines V_{in} explicitly only when I_ϵ does not depend upon V_{in}; however, substitution of Eq. 49 yields

$$V_{in}(T) = \int_0^T g_\epsilon(s)[V_\epsilon - V_{in}(s)]K(X_{in}, T - s; X_{in}) \, ds. \qquad (50)$$

This is a linear Volterra integral equation for $V_{in}(T)$. The equivalent steady-state equation is the linear algebraic equation appearing immediately before Eq. 32 in RR-I.

Solutions of Eq. 50 for particular transient $g_\epsilon(T)$ at particular locations must be obtained numerically. Barrett and Crill (1974) have computed such solutions. Equivalent computations for a compartmental model have been illustrated (Rall, 1967, Fig. 4). Here we summarize results obtained by numerical solution of Eq. 50 for the two cases of soma synaptic input location and dendritic terminal synaptic input location in our neuron model.

Our computations used the same neuron parameters as in the calculations for Figs. 3–7; here, we set $R_N = 1$ MΩ. The synaptic conductance time course was of the form given by Eq. 35 with $\alpha = 50$ and I_p replaced by 10^{-7} mho; hence the maximum conductance, attained at $T = 0.02$, was equal to 10^{-7} mho. When this $g_\epsilon(T)$ was applied to the soma, it resulted in a peak depolarization, peak $V_{in} \approx 0.0138 \, V_\epsilon$ at the soma. Note that for $V_\epsilon = 70$ mV, this peak $V_{in} \approx 1$ mV, which lies near the upper end of the experimental size range for a unitary (single terminal) somatic EPSP of cat spinal motoneurons (Iansek and Redman, 1973; see also Burke, 1967, and Kuno 1971). The fact that this peak V_{in}/V_ϵ is much smaller than unity implies that the synaptic driving potential remains also constant. Thus, the peak value of $I_\epsilon(T)$ was found to be 99% of the reference value obtained when V_{in} is replaced by zero in Eq. 49. Similarly, for this case, peak V_{in} was 99% of the reference value obtained when V_{in} is replaced by zero on the right in Eq. 50.

Greater effects were found when the same $g_\epsilon(T)$ was applied to a branch terminal. There, peak $V_{in} = 0.411 \, V_\epsilon$, which implies a very significant reduction of the synaptic driving potential, varying with time. The resulting synaptic current had its peak value reduced to 68.2% of its reference value; however, its time integral (the total input charge) was reduced to 67.2% of its reference value obtained when $V_{in} = 0$ in Eq. 49. The difference between the 68.2 and the 67.2% figures results from a slight distortion of the current time course; this is indicated also by a synaptic current peak time, $T = 0.014$, compared with a reference value of 0.02 for the input transient with $\alpha = 50$. It may be noted that with larger membrane depolarization at the input site, larger distortions of synaptic current should be expected to produce large discrepancies between the reduction in the current peak and the reduction in the total input charge.

The resulting EPSP at the soma for the above synaptic current at a dendritic terminal was computed by means of the response function at the soma for current injection at a branch terminal (Eqs. 33 and 34). This EPSP had a peak value of 0.00184 V_ϵ, which was 67.2% of its reference value, in agreement with the reduction of total input charge.[1] When this EPSP peak at the soma is compared with the peak $V_{in} = 0.411 \, V_\epsilon$ at the

---

[1] It is useful to know that the EPSP peak at the soma remains proportional to the total input charge at the branch terminal, even for slight changes in brief input time course.

branch terminal synaptic site, one obtains a peak voltage attenuation factor of 224 for this case. For those quantitatively inclined, one asks why this attenuation factor is 5% less than the factor of 235 found for the reference case of current injection. The answer is to be found in the fact that peak V_{in} (of 0.411 V_e) at the branch terminal was only 63.9% of its reference value, even though the time integral of $V_{in}(T)$ was 67.2% of its reference value. The difference between these 63.9 and 67.2% values results from a distortion of voltage time course that is revealed also by a voltage peak time, $T = 0.036$, at the branch terminal, compared with $T = 0.04$ for the reference case. When the input charge and the soma peak were both reduced to 67.2%, while the input peak was reduced to 63.9%, the attenuation factor becomes reduced from 235 to $(63.9/67.2)(235) = 224$.

It is instructive to briefly recapitulate this example of the several factors that effect the EPSP at the soma when a brief synaptic conductance transient is shifted from the soma to a branch terminal. Although the input resistance ratio, R_{BL}/R_N, is 15.5, the ratio of the voltage peaks at these two synaptic sites would be 46.3 (Fig. 6) if the input were current injection; however, because of synaptic conductance, this ratio of voltage peaks is reduced to about 30. Then the transient attenuation factor of 224 from the branch terminal to the soma results in an EPSP at the soma whose peak is less than one-seventh of that obtained with the same synaptic input at the soma.

Next, if we compare the charge delivered to and dissipated by the soma membrane in these two cases, the difference appears smaller. We have already noted that the synaptic conductance transient at the branch terminal delivered only 67.2% of the reference input charge. From Fig. 7, we are reminded that 8.5% of the actual input charge will be dissipated at the soma designated there; the result is $(8.5)(0.672) = 5.7\%$ of the reference input charge. For synaptic input at the soma, 99% of the reference input charge was delivered, and of this, 12.7% can be shown to be the portion dissipated at the same designated soma; this is about 12.6% of the reference input charge. Therefore, the ratio, $5.7/12.7 \simeq 0.45$ tells us that the amount of charge dissipated at the soma for the synaptic input at the branch terminal is almost half that dissipated at the soma for the synaptic input at the soma. This is in general agreement with estimates that Barrett and Crill (1974) obtained for their example. There is no contradiction between the charge dissipation ratios and the voltage peak ratios; the difference results from the fact that the EPSP for somatic input has an earlier and larger voltage peak, while that for distal dendritic input is slower with a later, more flattened and lower voltage peak (cf. illustrations in Rall 1962, 1964, 1967).

We conclude with a simple example illustrating nonlinear summation of transient EPSPs. This phenomenon results from the reduction in driving potential caused by the proximity in time and/or spatial location of multiple synaptic events. The consequence for simultaneous dendritic conductance inputs is that the EPSP seen at the soma does indeed depend on how the synaptic conductance transient is distributed between the branches. This is not the case for current inputs. Consider the above example. If the synaptic conductance g_e is shared equally by the eight branch terminals of one tree, the peak g_e is 1.25×10^{-8} mho for each terminal and very little reduction

in synaptic driving potential is found. The peak value of I_ϵ is 94% of its reference value. The resulting EPSP at the soma is also reduced to 94% of the reference value.[1] This contrasts with the previous example of EPSP reduction to 67% when the synaptic input (conductance transient) was all placed on a single branch. This provides one more specific illustration of this transient phenomenon which has been previously discussed and illustrated (Rall, 1964, 1967, 1970). Nonlinear summation of synaptic input occurs when the individual synapses cause significant membrane depolarization (reduction of synaptic driving potential) at the time and place of the other synaptic inputs. Questions related to this phenomenon have also been addressed by Iansek and Redman (1973).

SUMMARY

(a) Analytic expressions are obtained for the response function corresponding to an instantaneous pulse of current injected to a single dendritic branch in a branched dendritic neuron model. In the main text these results are derived under strict assumptions of symmetry; more general results are provided in the Appendix. The dendritic membrane is assumed passive and the branching satisfies the 3/2-power law. The response function is obtained by a superposition technique using component response functions. This technique was described for the corresponding steady state problem in (Rall and Rinzel, 1973). Each component response function has two different series representations: one converges better as $T \rightarrow \infty$; the other as $T \rightarrow 0$. These alternate representations are used to analyze the small time and large time behavior of the response function.

(b) The voltage transients at various points in the dendritic tree for a brief current injection at a terminal branch were computed using the response function in a convolution formula (Eq. 5); these transients are illustrated in Figs. 4 and 5. The attenuation and delay characteristics of the depolarization peak as it spreads throughout the neuron model are summarized in Table I.

(c) Because the system is linear, the transient depolarization seen at the soma is independent of the way in which a given current input might be shared among several branches provided the input locations are (electrotonically) equidistant from the soma.

(d) In general, the peak depolarization for a given current injection is not proportional to the input resistance at the injection site. An example, which compares a branch terminal site with a soma site, is presented to illustrate this point. For this case, the ratio of depolarization peaks, for a brief current input, very nearly equals $N2^M$, the ratio of the input resistance of the input branch extended as a semi-infinite cylinder to the input resistance of the parallel combination of all the dendritic trunks extended as semi-infinite cylinders.

(e) While there is severe attenuation of voltage transients from branch input sites to the soma, the fraction of total input charge actually delivered to the soma and other trees is about one-half. This fraction is independent of the input time course. The calculation of the fraction of charge dissipated in various portions of the dendritic tree is outlined and an example is illustrated by Fig. 7.

(*f*) When synaptic input is represented as a conductance change, it is important to consider the reduction in the effective synaptic driving potential caused by membrane depolarization at the input site. This is taken rigorously into account by Eqs. 49 and 50. For any given input site and given synaptic conductance time course, one can compute both a reference voltage transient (assuming $V_{in} = 0$ in Eq. 50, right-hand side), and the actual reduced voltage transient defined by Eq. 50. An illustrative example showed the peak synaptic current at the branch terminal reduced to 68% of the reference value, the total input charge reduced to 67% of reference, the local voltage peak reduced to 64% of reference, and the EPSP peak at the soma reduced to 67% of reference. In contrast, the same synaptic conductance input at the soma resulted in 99% of reference synaptic current and 99% of reference EPSP.

APPENDIX

Generalizations

In the Appendix of RR-I we provided the steady-state solutions to a variety of problems with relaxed assumptions of symmetry and input location. Here we consider some analogous transient problems. In each case we give the Laplace transformed response functions. For Eqs. 51–53, 55, and 56, the appropriate time domain expressions can be found by using the addition formulas for the hyperbolic functions along with the component response function inversions (Eqs. 21, 22, 24 and 25). We do not present derivations of the solutions to the problems considered below. Rather, we obtain the Laplace transformed response functions for a given problem from the corresponding steady-state solution for maintained unit current injection, $I = 1$, as follows. We replace the argument Z of any hyperbolic function by qZ and then multiply the entire steady-state solution by q^{-1}. This formal procedure is based on the observation that under the change of variable $Y = qX$, the transformed transient problem for the response function becomes a steady-state problem with steady current source q^{-1}. If one prefers to derive these results, the discussion which accompanies the solution of the steady-state problems in RR-I is applicable here also.

Effect of Input Site Not Restricted to X = L

Suppose the site of current injection is located at a distance X_{in} from the origin on a branch of order k_i so that $X_{k_i} \leq X_{in} \leq X_{k_{i+1}}$. Then the response function $K(X, T; X_{in})$ is obtained from RR-I, Eq. A 7, by following the above recipe. If we use the component response functions 17 and 18, we can express the solution in the input branch, for $X_{k_i} \leq X \leq X_{in}$, as

$$\tilde{K}(X, p; X_{in}) = \cosh[q(L - X_{in})]\left[N^{-1}\tilde{K}_{ins}(X, L, p)\right.$$
$$\left. + (N - 1)N^{-1}\tilde{K}_{clp}(X, L, p) + \sum_{k=1}^{k_i} 2^{(k-1)}\tilde{K}_{clp}(X - X_k, L - X_k, p)\right] \quad (51)$$

The response function, evaluated at $X = 0$, takes the reduced form

$$\tilde{K}(0, p; X_{in}) = N^{-1}\cosh[q(L - X_{in})]\tilde{K}_{ins}(0, L, p). \quad (52)$$

In the special case when $X_{in} = 0$, this can be written (using Eq. 17)

$$\tilde{K}(0, p; 0) = N^{-1}\tilde{K}_{\mathrm{ins}}(L, L, p). \tag{53}$$

Thus, for example, the small T representation follows from Eq. 24 as

$$K(0, T; 0) = \frac{R_{T\infty}e^{-T}}{N(\pi T)^{1/2}} \sum_{n=-\infty}^{\infty} \exp[-(2nL)^2/4T]. \tag{54}$$

Effects of Unequal Trunks and Branches

To treat the case in which the trunks and branches of the trees are not equal in diameter we refer to notation introduced in RR-I. The ratio of the summed $d^{3/2}$ value (for all trunks) to the $d^{3/2}$ value of the trunk of the input tree is denoted by γ. For a kth order branch point, γ_k is the ratio of the parent $d^{3/2}$ value to the $d^{3/2}$ value of the input carrying daughter branch. Now suppose all the trees have the same electrotonic length L. Then, in analogy with RR-I, Eq. A 9, the transformed response function for $X_{k_i} \leq X \leq X_{in}$ is

$$\tilde{K}(X, p; X_{in}) = \cosh[q(L - X_{in})][\gamma^{-1}\tilde{K}_{\mathrm{ins}}(X, L, p)$$

$$+ (1 - \gamma^{-1})\tilde{K}_{\mathrm{clp}}(X, L, p) + \sum_{k=1}^{k_i} p_k\tilde{K}_{\mathrm{clp}}(X - X_k, L - X_k, p)], \tag{55}$$

where $p_1 = \gamma_1 - 1, p_2 = \gamma_1(\gamma_2 - 1), \ldots, p_k = \gamma_1\gamma_2\ldots(\gamma_k - 1)$. At the origin we have

$$\tilde{K}(0, p; X_{in}) = \gamma^{-1}\cosh[q(L - X_{in})]\tilde{K}_{\mathrm{ins}}(0, L, p). \tag{56}$$

In the case where the trees are not restricted to have the same length, the expressions 55 and 56 apply provided we replace γ by

$$\gamma = \left[\sum_j d_j^{3/2}\tanh(qL_j)\right]/[d_{in}^{3/2}\tanh(qL_{in})], \tag{57}$$

where the subscript "in" refers to the input tree. Implicit in the component response functions is a value for R_∞ which should be taken equal to the $R_{T\infty}$ value for the input tree.

REFERENCES

BARNWELL, G. M., and B. J. CERIMELE. 1972. *Kybernetik.* **10**:144.

BARRETT, J. N., and W. E. CRILL. 1974. *J. Physiol. (Lond.).* **239**:301, 325.

BURKE, R. E. 1967. *J. Neurophysiol.* **30**:1114.

CARSLAW, H. S., and J. C. JAEGER. 1959. Conduction of Heat in Solids. Oxford Press, London. 510.

FATT, P., and B. KATZ. 1951. *J. Physiol. (Lond.).* **115**:320.

IANSEK, R., and S. J. REDMAN. 1973. *J. Physiol. (Lond.).* **234**:665.

JACK, J. J. B., and S. J. REDMAN. 1971 *a. J. Physiol. (Lond.).* **215**:283.

JACK, J. J. B., and S. J. REDMAN. 1971 *b. J. Physiol. (Lond.).* **215**:321.

KATZ, B., and R. MILEDI. 1963. *J. Physiol. (Lond.).* **168**:389.

KATZ, B., and S. THESLEFF. 1957. *J. Physiol. (Lond.).* **137**:267.

KUNO, M. 1971. *Physiol. Rev.* **51**:657.

LUX, H. D. 1967. *Pflügers Arch.* **297**:238.

MACGREGOR, R. J. 1968. *Biophys. J.* **8**:305.

NORMAN, R. S. 1972. *Biophys. J.* **12**:25.

RALL, W. 1960. *Exp. Neurol.* **2**:503.

RALL, W. 1962. *Ann. N. Y. Acad. Sci.* **96**:1071.

RALL, W. 1964. *In* Neural Theory and Modeling. R. F. Reiss, editor. Stanford University Press, Stanford, Calif. 73.

RALL, W. 1967. *J. Neurophysiol.* **30**:1138.

RALL, W. 1969. *Biophys. J.* **9**:1483.

RALL, W. 1970. *In* Excitatory Synaptic Mechanisms. P. Anderson and J. K. S. Jansen, editors. Universitets Forlaget, Oslo. 175.

RALL, W., and J. RINZEL. 1973. *Biophys. J.* **13**:648.

REDMAN, S. J. 1973. *J. Physiol. (Lond.).* **234**:637.

ROBERTS, G. E., and H. KAUFMAN. 1966. Table of Laplace Transforms. Saunders, Philadelphia. 367.